Evaporation of Water through Butanol Films at the Surface of Supercooled Sulfuric Acid

Jennifer R. Lawrence, Samuel V. Glass, and Gilbert M. Nathanson*

Department of Chemistry, University of Wisconsin−Madison, 1101 University Avenue, Madison, Wisconsin 53706

Received: January 4, 2005; In Final Form: April 29, 2005

The evaporation of water was monitored from 60, 64, and 68 wt % D_2SO_4 at 213 K containing 0−0.18 M 1-butanol. Measurements were performed in vacuum using a mass spectrometer to record the velocities and relative fluxes of the desorbing D_2O. In addition, the surface activity of butanol in the acid was characterized by hyperthermal argon atom scattering in conjunction with surface tension and butanol evaporation measurements. The segregated butyl species reach surface concentrations of $\sim 4 \times 10^{14}$ cm^{-2} (∼80% surface coverage) at 0.18 M bulk concentration. We find that the butyl films do not impede the evaporation of D_2O from the acid to within the 5% uncertainty of the measurements. This result implies that small, soluble surfactants such as butanol form porous films that will not alter the growth or shrinkage of supercooled sulfuric acid droplets in the atmosphere.

Introduction

When hexadecanol is spread on water, the rate of water evaporation decreases by 4 orders of magnitude.[1,2] This dramatic reduction occurs because the hydrocarbon chains pack together tightly at the surface and impede water transport through the monolayer. The resistance to gas permeation increases exponentially with surfactant chain length for alcohols and fatty acids ranging from 14 to 22 carbon atoms.[1,3] Very little, however, is known about gas transport through short-chain surfactants such as butanol. These shorter molecules are likely to form less compact films because of weaker cohesive forces among the hydrocarbon chains. Short-chain surfactants are also much more soluble in acidic and aqueous subphases and generally do not undergo the phase transitions to compact structures that are characteristic of long-chain molecules.[4] In this paper, we investigate the evaporation of water from pure and butanol-doped sulfuric acid at concentrations from 60 to 68 wt % D_2SO_4 at 213 K. In the following companion paper, we explore the effects of butanol films on the uptake of HCl, HBr, and CF_3CH_2OH in the cold acid. Our results show that the butanol surfactant has no measurable effect on the evaporation of D_2O or on the uptake of CF_3CH_2OH even at nearly monolayer butanol coverages. Even more surprisingly, the butanol film is found to enhance the entry of HCl and HBr into sulfuric acid.

The choice of supercooled sulfuric acid as the subphase liquid was motivated by the role of sulfuric acid particles in heterogeneous reactions in the atmosphere.[5] These submicron droplets range in composition from 40 to 80 wt % H_2SO_4 at 200 to 240 K in the lower stratosphere[6] and over a wider range of acidities in the upper troposphere.[7] Field studies indicate that upper tropospheric particles often contain organic material,[8−11] implying that some particles may be coated with surface-active organic molecules. These organic coatings have the potential to affect rates of droplet growth (by reducing water evaporation and condensation rates) and the rates and outcomes of heterogeneous reactions that occur in the interfacial and bulk regions of these droplets (by altering gas uptake rates and introducing gas−surfactant reactions).[5,12−17] While aerosols in the lower troposphere contain a variety of long-chain surfactants,[12] we focus on the permeation resistances posed by short-chain species, which are more likely to be found in aerosols in the upper troposphere.[5,18] In particular, this paper presents studies of the evaporation of D_2O from supercooled deuterated sulfuric acid solutions containing small concentrations of the model soluble surfactant 1-butanol(D), $CH_3CH_2CH_2CH_2OD$, referred to below as BuOD.

In the absence of gas-phase diffusion, the flux of molecules entering a liquid can be expressed as $J_{enter} = \alpha\langle v\rangle n_{gas}/4$, where $\langle v\rangle$ is the mean thermal velocity of the gas, n_{gas} is the density of gas molecules far from the surface, and α is the probability that the gas molecule enters the liquid upon striking the surface (also known as the mass accommodation, condensation, or sticking coefficient).[19,20] Equivalently, α may be measured in evaporation experiments by equating the evaporation and condensation fluxes at equilibrium. The effect of a surfactant in reducing gas permeation is often expressed in terms of the resistance r_{surf} posed by the surfactant, where $r_{surf} = 4/(\alpha\langle v\rangle)$.[21] For hexadecanol on water at 298 K at its equilibrium spreading pressure, r_{surf} is found to be $\sim$1.5 s cm^{-1}, corresponding to $\alpha \sim 4.5 \times 10^{-5}$, a 20000-fold reduction in water evaporation assuming unimpeded evaporation from the bare liquid.[1]

Early experiments on water permeation through surfactants were carried out by measuring the amount of water evaporating into a desiccant suspended above a trough containing water and a long-chain surfactant.[1,22,23] This technique, however, cannot easily be extended to measure the small resistances likely posed by short-chain surfactants because of the large resistance of the stagnant air layer between the liquid and desiccant. The resistance of this air layer is typically $\sim$1 s cm^{-1}, limiting measurements of α to values smaller than 10^{-3} for a 10% change in evaporation rate between the bare and surfactant-coated liquids. Our vacuum experiments are conducted at pressures below 10^{-3} Pa (10^{-5} Torr),[24,25] enabling D_2O evaporation rates from the pure and butanol-doped acid to be compared to within the 5% reproducibility of our measurements.

* Corresponding author. E-mail: nathanson@chem.wisc.edu.

10.1021/jp050042f CCC: $30.25
Published on Web 08/02/2005

In addition to extensive studies of gas transport through films on water,[2,23] permeation rates have also been measured for strongly acidic subphases. Hexadecanol monolayers on 45−95 wt % phosphoric acid droplets were found to reduce water evaporation and condensation by 10000-fold at the lower acid concentrations, but the resistance decreased by a factor of 4 at higher acidities due to protonation of the alcohol and expansion of the film.[26] Films of hexadecanol and fatty acids ranging in thickness from one monolayer to several nanometers have also been found to reduce the uptake of ammonia[27] and water[28] into sulfuric acid aerosols.

Several gas permeation and uptake experiments have been performed with soluble surfactants. Resistances of 1.5−6.0 s cm^{-1} were measured for CO_2 uptake through C_{12} to C_{16} ionic surfactants,[29] and nonanol[30] and decanol[31,32] films were each observed to reduce water uptake. 1- and 4-octanol films on water were found to reduce CO_2 uptake,[33] but a dilute, 0.2 monolayer film of 1-octanol on water had no apparent effect on the uptake of acetic acid.[34] A recent study of water evaporation through long-chain soluble surfactants into air was unable to detect any surface resistance, implying that α must be larger than 10^{-3}.[35] These studies have been complemented by molecular dynamics simulations of the uptake of gaseous methanol into methanol−water solutions.[36] The simulations predict almost no surface resistance ($\alpha_{methanol} > 0.97$) into solutions from neat methanol to neat water. Organic films may also enhance uptake when the gas species is more soluble in the surface film than in the subphase, as recently shown for the adsorption of pyrene and anthracene onto 1-octanol-coated water.[37]

The work described above suggests that high-coverage films of short-chain alcohols might impede gas transport, but not significantly enough to be measured in air (where it is difficult to measure values of α larger than $\sim 10^{-3}$). An extrapolation of the chain length dependence of C_{14} to C_{22} normal alcohols on water predicts that 1-butanol would lower the evaporation rate by a factor of 100.[1,2] We find, however, that the addition of butanol does *not* reduce the evaporation of D_2O into vacuum from 60−68 wt % D_2SO_4 at 213 K by more than our uncertainty of 5%. As discussed below, these results imply that short-chain surfactants such as butanol form porous films on sulfuric acid droplets that do not impede water transport.

Properties of Pure and Butanol-Doped Sulfuric Acid Solutions

Sulfuric acid solutions composed of 60−68 wt % D_2SO_4 that are supercooled to 213 K possess high viscosities (400−1800 cP), low water vapor pressures (0.1−0.03 Pa), and high water vaporization enthalpies (51−54 kJ mol^{-1}).[6,38,39] They are formally 0.23−0.30 mole fraction D_2SO_4, but the acid ionizes extensively and consists of D_2O, D_3O^+, DSO_4^-, and SO_4^{2-}.[6,40] Sum frequency generation experiments using H_2SO_4 solutions indicate that the interfacial region is composed of ion pairs or neutral molecules with no dangling OH bonds.[41−43] Surface tension[41] and Auger electron spectroscopy[44] studies further indicate that there is little or no surface segregation of water or acid species.

Alcohols are readily protonated in sulfuric acid, and ^{13}C NMR measurements indicate that methanol, ethanol, and propanol reach half-protonation in 76−78 wt % H_2SO_4 solutions at room temperature.[45,46] Butanol may also form butyl hydrogen sulfate and sulfate anions ($BuOSO_3H$ and $BuOSO_3^-$),[47] but Iraci et al. concluded that esterification rates of methanol with 45−70 wt % H_2SO_4 solutions are drastically reduced at low temperatures.[48,49] On the basis of their analysis, we estimate that less than 10% of the butanol in our experiments is converted to $BuOSO_3D$ and $BuOSO_3^-$, leaving 90% or more as BuOD and $BuOD_2^+$.

We previously characterized the surface properties of 0−72 wt % H_2SO_4 solutions doped with BuOH using surface tension measurements.[50] These studies show that the surface tensions drop from 72−75 dyn cm^{-1} for the pure solutions to 39−45 dyn cm^{-1} for 0.4 M butanol solutions at 294 K. A Gibbs adsorption analysis yields the total butyl surface excess, which is the sum of all BuOH, $BuOH_2^+$, $BuOSO_3H$, and $BuOSO_3^-$ species that segregate in the interfacial region. If these excess species segregate solely to the outermost surface layer, then the computed surface excess is equal to the total surface coverage to within 2% because of the low concentration of butyl species in the 0−0.4 M bulk solution. We find that this coverage reaches saturation values near 0.2 M butanol, which for 58 wt % H_2SO_4 at 294 K is 2.5×10^{14} cm^{-2} (∼50% of maximum coverage based on a molecular area of ∼20 Å^2 for close-packed long-chain alcohols[51]). This coverage drops to 1.9×10^{14} cm^{-2} (∼40% of a monolayer) on 72 wt % H_2SO_4 at 294 K, but rises to $\sim 3.6 \times 10^{14}$ cm^{-2} (∼70% of a monolayer) at 208 K. These results suggest that conversion of BuOH to $BuOH_2^+$ at higher acid concentrations causes the butyl groups to pack more loosely because of charge repulsion among the headgroups, while lower temperatures increase the cohesive forces among the chains. On the basis of these results, we expect that butyl films on the 60 wt % D_2SO_4 solutions at 213 K used in the present experiments reach a density exceeding 4×10^{14} cm^{-2} (∼80% of a fully packed monolayer), corresponding to an average molecular area smaller than 25 Å^2. Preliminary surface tension measurements of butanol on 62 wt % H_2SO_4 at 210 K confirm this prediction.

Experimental Procedure

Figure 1 depicts the scattering apparatus and sulfuric acid reservoir. Continuously renewed, vertical acid films are created by rotating a 5.0 cm diameter glass wheel partially submerged in 60 mL of sulfuric acid at rates of 0.083−0.83 Hz.[24,52] A cylindrical Teflon scraper skims away the outer ∼0.1 cm of acid to remove insoluble surface-active impurities and to ensure that the surface of the film is positioned precisely in the interaction region. The remaining ∼0.05 cm thick acid film then moves in front of a 0.60 cm^2 circular hole, where it is intercepted by the molecular beam. At a typical rotation speed of 0.17 Hz, the time between scraping and appearance at the edge of the hole is $t_{rep} = 0.49$ s. As shown later, this replenishment time allows the butanol film to be reestablished at the surface of the acid. The acid remains in front of the hole for $t_{open} = 0.45$ s and is exposed to the molecular beam for $t_{exp} = 0.25$ s.

The acid solutions are prepared by diluting 98 wt % D_2SO_4/D_2O with D_2O, adding BuOD, and then cooling to 213 ± 1 K. All reagents (Aldrich) are used without further purification. The pressure in the scattering chamber rises to (3−8) × 10^{-4} Pa for 68−60 wt % D_2SO_4, respectively. Titrations show that the acid concentration changes by no more than 0.5 wt % over a 5 day period.

The evaporation of D_2O ($m/z = 20$) and BuOD ($m/z = 56$) is monitored by a differentially pumped mass spectrometer oriented at $\theta_{fin} = 45°$ with respect to the acid film.[24] The desorbing molecules are chopped into 38 μs pulses by a spinning slotted wheel and travel a distance $d_{post} = 18.4$ cm to the mass spectrometer, where their arrival times are recorded in 2 μs intervals.

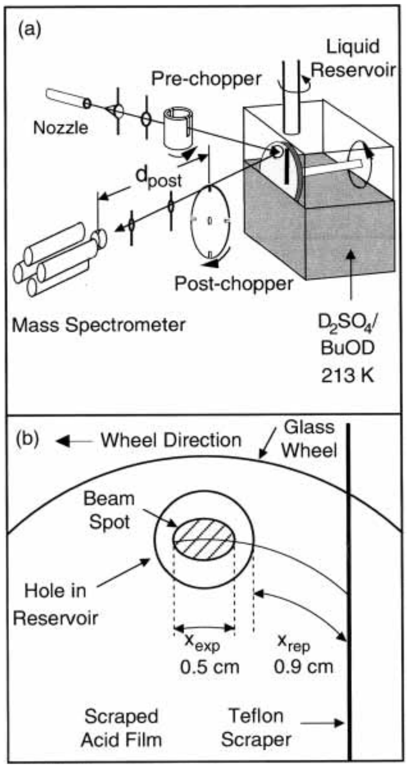

Figure 1. (a) Schematic diagram of the scattering apparatus. The liquid reservoir is sealed except for a 0.88 cm diameter hole centered at the interaction region. (b) Expanded view of the front face of the liquid reservoir. The argon beam enters the hole from the left at $\theta_{inc} = 45°$.

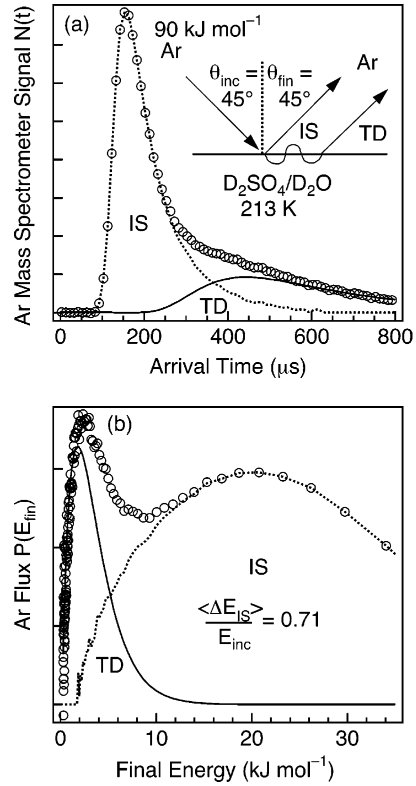

Figure 2. (a) Time-of-flight (TOF) spectrum of Ar scattering from 60 wt % D_2SO_4 at 213 K. "IS" and "TD" refer to direct inelastic scattering and thermal desorption. The solid curve is a 213 K Maxwell–Boltzmann fit to the TD component. (b) Energy distribution obtained by direct inversion of the spectrum in panel a. $\langle \Delta E_{IS}\rangle/E_{inc} = (E_{inc} - \langle E_{IS}\rangle)/E_{inc}$ is the average fractional energy transfer in the IS channel.

Beams of ~90 kJ mol^{-1} argon atoms are generated by expanding a 2% Ar/H_2 mixture through a 0.13 mm diameter glass nozzle at 1 bar total pressure. The atomic beam strikes the acid film at an incident angle of $\theta_{inc} = 45°$ and projects a 0.35 cm × 0.50 cm elliptical spot on the acid surface. The exiting Ar atoms are detected at $m/z = 40$ at $\theta_{fin} = 45°$.

Results and Analysis

Argon Scattering from Bare and Butyl-Coated Sulfuric Acid. Hyperthermal argon atom scattering is used to monitor and characterize butyl species that segregate to the surface of sulfuric acid in vacuum. Figure 2a shows a time-of-flight (TOF) spectrum of 90 kJ mol^{-1} argon scattering from bare 60 wt % D_2SO_4 at 213 K at $\theta_{inc} = 45°$. The signal is proportional to the number density $N(t)$, which is used to calculate the relative flux or probability $P(E_{fin})$ that an argon atom scatters with energy E_{fin} at $\theta_{fin} = 45°$. The translational energy distribution, determined from the relations $E_{fin} = (1/2)m_{Ar}(d_{post}/t)^2$ and $P(E_{fin}) \sim [N(t)]t^2$, is shown in Figure 2b. The bimodal spectrum illustrates the two pathways available to the impinging Ar atoms. The narrow peak at early arrival times (high exit energies) corresponds to those atoms that undergo direct inelastic scattering (IS), on average transferring 71% of their incident energy to the acid during one or a few collisions before leaving the surface. The broader peak at later arrival times (low exit energies) corresponds to Ar atoms that become momentarily trapped in the interfacial region and then thermally desorb (TD). This region of the spectrum can be fit with a Boltzmann distribution, $P_{TD}(E_{fin}) = E_{fin}(RT_{acid})^{-2} \exp(-E_{fin}/RT_{acid})$, constrained such that the peak of the IS component is set to 0 at $RT_{acid} = 1.8$ kJ mol^{-1}.

Figure 3 demonstrates that hyperthermal argon scattering is very sensitive to the presence of butyl species at the surface of 60 wt % D_2SO_4. As the BuOD concentration is increased from 0 to 0.18 M, the IS channel sharply diminishes in size and shifts to later arrival times. These changes indicate that fewer Ar atoms scatter at the specular angle and that those Ar atoms that do scatter transfer more of their incident energy to the surface before recoiling away. Concurrently, the TD signal grows upon addition of BuOD, indicating that more Ar atoms thermalize on the surface with increasing butanol concentration. The effects of added butanol appear to be most dramatic at low concentrations and begin to level off at approximately 0.04 M BuOD.

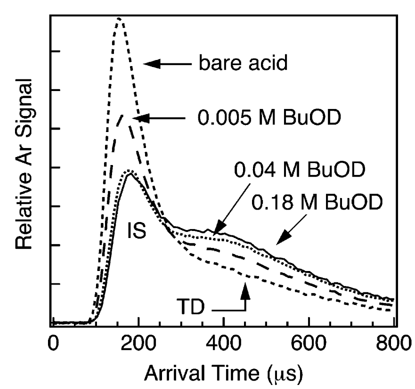

Figure 3. TOF spectra of 90 kJ mol^{-1} Ar scattering from 60 wt % D_2SO_4 containing 0 (---), 0.005 (– –), 0.04 (···), and 0.18 M (—) butanol. The spectra are not normalized. They initially change sharply with the addition of butanol, followed by smaller changes at higher BuOD concentrations.

The changes in the argon IS and TD components mirror the surface concentration of butyl species determined by surface tension measurements, as shown in Figure 4.[50] This surface

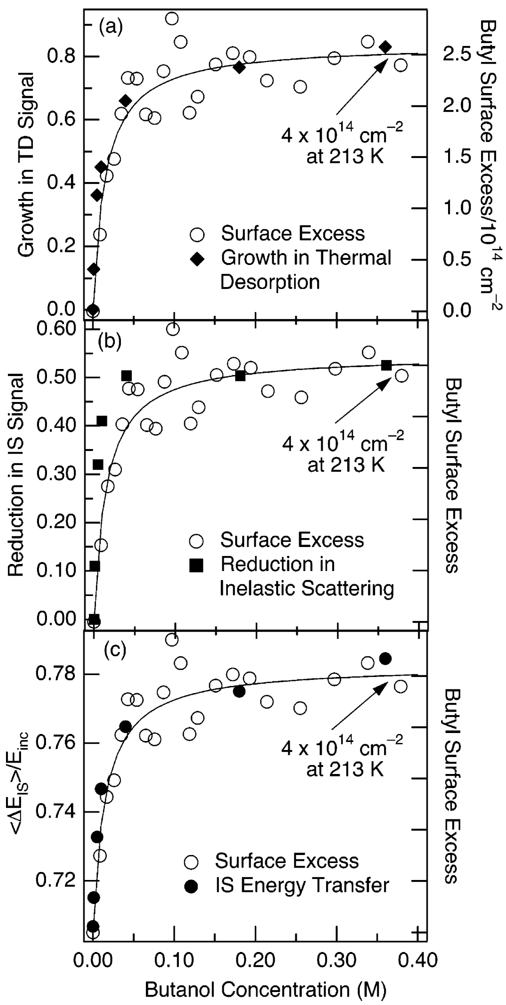

Figure 4. (a) Fractional growth in Ar TD signal versus BuOD concentration in 60 wt % D_2SO_4 at 213 K. The butyl surface excess, calculated from surface tension measurements of butanol in 58 wt % H_2SO_4 at 294 K,[50] is plotted on the right axis. The solid curve is a fit using the Langmuir adsorption equation. Additional measurements show that the maximum butyl surface coverage rises from 2.5×10^{14} to 4×10^{14} cm^{-2} as the temperature is lowered from 294 to 213 K. (b) Fractional reduction in the peak IS signal versus BuOD concentration. (c) Average fractional energy transfer in the IS channel versus BuOD concentration. In each panel, the solid point furthest to the right was measured at a butanol concentration of 1.0 M, but is shown at a concentration of 0.36 M. The uncertainties are $\pm 0.3 \times 10^{14}$ cm^{-2} in the surface excess and ±5% of full scale in the argon scattering parameters.

excess curve (open circles) is similar in shape at acid concentrations from 0 to 72 wt % H_2SO_4 and at 294 and 208 K, and is shown here for 58 wt % H_2SO_4 at 294 K. In every case, the surface excess follows a Langmuir-type adsorption curve, rising rapidly at low bulk butanol concentrations and then plateauing near 0.2 M. The three panels in Figure 4 depict in detail how the growth in thermal desorption (top panel), reduction in inelastic scattering (middle panel), and shift in energy transfer (bottom panel) of the impinging argon atoms mimic the butyl surface excess. In each case, the trends in Ar scattering track the initial, rapid rise and then slow increase in butyl surface coverage. The overlap between the Ar scattering patterns and the surface excess curves is our most direct evidence that the surface concentration of butyl species is the same when the film is prepared using a continuously renewed, vertical wheel in a vacuum and using a static, horizontal film in air. This conclusion is further justified by the BuOD evaporation measurements described in the next section.

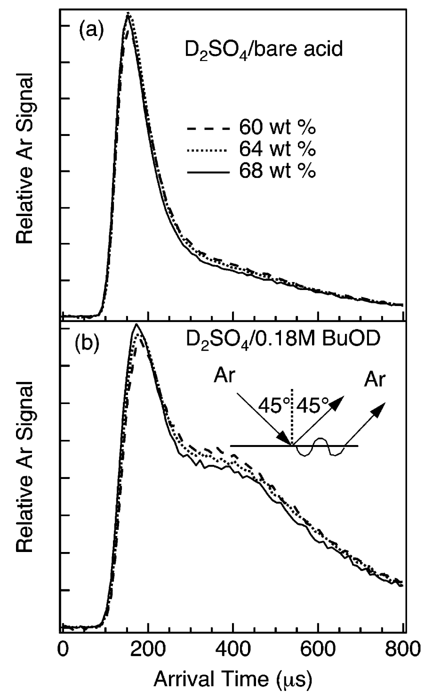

Figure 5. TOF spectra of 90 kJ mol^{-1} Ar scattering from 60, 64, and 68 wt % D_2SO_4 at 213 K: (a) bare acid and (b) 0.18 M BuOD. The vertical scale is different in each panel.

Argon scattering measurements also show that the butyl species are surface active in 64 and 68 wt % D_2SO_4. Figure 5 compares collisions of argon atoms with bare acid and 0.18 M BuOD solutions at three acid concentrations. The top panel shows that the TOF spectra change only slightly from bare 60 to 68 wt % D_2SO_4, indicating that hyperthermal Ar scattering is not very sensitive to the 10 mol % increase in SO_4 species at the surface. The spectra in the lower panel recorded from the butanol-doped solutions are also similar in size and shape, but as in Figure 3 they are very different from the bare acid spectra. The similarity among the spectra in panel b confirm that butyl species also segregate to the surfaces of 64 and 68 wt % acid at 213 K, a result consistent with surface tension measurements at 294 K.[50]

Butanol Evaporation. Butanol evaporation measurements provide a window into the surface and subsurface regions of the acid solutions. After the acid-coated wheel is skimmed by the Teflon scraper, the butyl concentration at the surface of the acid is equal to its bulk value. The different butyl species diffuse randomly through the acid, but they collect preferentially at the surface because their free energy is lowest there. This segregation depletes the region just below the surface, which refills as molecules continue to diffuse from the bulk.[53,54] The equilibrium evaporation flux of a 0.2 M butanol solution in 60 wt % D_2SO_4 at 213 K corresponds to ~10 monolayers per second, based on an estimated solubility of ~10^7 M atm^{-1}.[55] This final butanol evaporation flux will not be reestablished until the subsurface and surface butyl concentrations reach their steady-state values. Thus, the measurement of a steady, maximum BuOD evaporation flux implies that the surface and subsurface regions must each be close to their terminal concentrations. We therefore measured the BuOD evaporation rate as a function of replenishment time t_{rep} and bulk BuOD concentration in order to determine at which t_{rep} the butyl film and subsurface region are repopulated on the acid-covered wheel.

Figure 6 displays butanol evaporation spectra for 0.005−0.18 M BuOD in 60 wt % D_2SO_4 at times t_{rep} = 0.49 and 0.10 s.

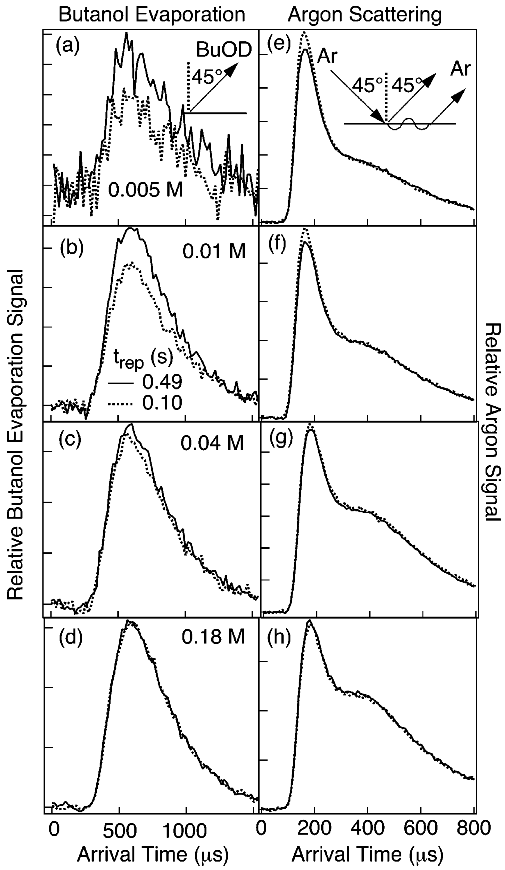

Figure 6. (a)−(d) TOF spectra of butanol evaporation at replenishment times t_{rep} = 0.49 (—) and 0.10 s (···) from 60 wt % D_2SO_4 containing 0.005, 0.01, 0.04, and 0.18 M BuOD. (e)−(h) TOF spectra of 90 kJ mol^{-1} Ar scattering at the same BuOD concentrations and replenishment times. The vertical scale is different in each panel.

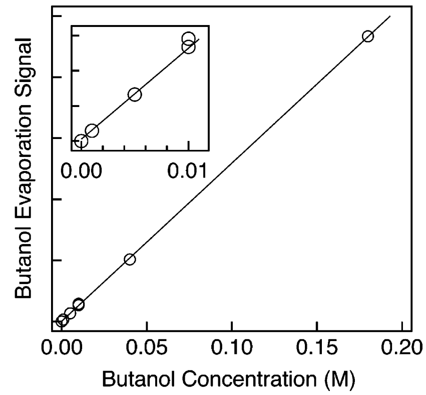

Figure 7. BuOD evaporation signal versus butanol concentration in 60 wt % D_2SO_4. The replenishment time (t_{rep}) is 0.49 s. The inset is an expanded view of the butanol evaporation signal at low butanol concentration.

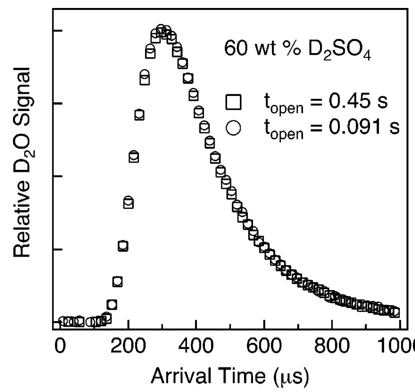

Figure 8. TOF spectra of D_2O evaporation from 60 wt % D_2SO_4 at different times for the patch of acid open to the vacuum: t_{open} = 0.45 (□) and 0.091 s (○).

For the most dilute (0.005 M) butanol solutions, the signal recorded at t_{rep} = 0.10 s is about two-thirds the signal recorded at 0.49 s. This result indicates that 0.10 s is not long enough for the butyl species to diffuse to the surface after the acid-coated wheel is skimmed by the scraper. The signal at t_{rep} = 1.0 s (not shown) is just slightly higher than that at 0.49 s, indicating that the subsurface and surface regions of the 0.005 M solution are mostly refilled 0.49 s after scraping. At higher butanol concentrations, less time should be required to replenish the butanol, and the desorption signal from the 0.04 M solution (panel c) varies little with t_{rep}. No variation is observed for the 0.18 M BuOD solution, confirming that the subsurface and surface butanol concentrations are reestablished within the fastest replenishment time of 0.10 s.

The change in butyl surface coverage itself with t_{rep} can be monitored with argon scattering, as shown in the right-hand panels of Figure 6. At the lower butanol concentrations, the reduction in the IS component is larger at t_{rep} = 0.49 s, which is characteristic of surfaces containing more butanol (the changes in the TD channel are too small to be observable). As the bulk butanol concentration increases, the difference in IS signal with t_{rep} diminishes and at 0.18 M the Ar spectra at t_{rep} = 0.49 and 0.10 s are the same. In all cases, we find that the Ar scattering and butanol spectra are nearly identical at t_{rep} = 0.49 and 1.0 s (not shown). The Ar scattering and butanol evaporation results collectively indicate that the surface and subsurface regions of the acid become saturated with butyl species over a time $t_{rep} \approx$ 0.5 s at all butanol concentrations. In the Appendix, this quick replenishment time is shown to be at least as fast as predicted by quiescent diffusion models, suggesting that there is little or no barrier to the adsorption of butyl species from solution to the surface.

A final test of butanol segregation is shown in Figure 7. This graph displays the integrated BuOD evaporation signal at t_{rep} = 0.5 s against bulk butanol concentrations of 0.001−0.18 M. The points are fit well by a straight line passing through the origin, indicating that these butanol concentrations lie within the Henry's law limit. This linearity confirms that the surface and subsurface regions are replenished even at the lowest concentrations, for otherwise the evaporation signal would not be proportional to the bulk concentration. The observed linearity further implies that the butyl surface layer does not impede evaporation of the butanol itself, as might occur at high surface concentrations if the butyl species orient and pack tightly together. An identical conclusion was reached from molecular dynamics simulations that found that methanol enters unimpeded into methanol−water solutions.[36]

Water Evaporation. D_2O molecules continuously evaporate from the acid on the rotating wheel at rates of 1000−200 monolayers s^{-1} for 60−68 wt % D_2SO_4, respectively, at 213 K (these rates are 100−20 times higher than the butanol evaporation rates for 0.2 M solutions). We must therefore show that the interface does not become more acidic or evaporatively cool because of D_2O evaporation during the 0.45 s interval that the acid is open to the vacuum. This is demonstrated in Figure 8, which compares D_2O evaporation spectra at open times of 0.09 and 0.45 s for 60 wt % D_2SO_4. The spectra are identical in intensity and in shape, indicating that water from the bulk readily

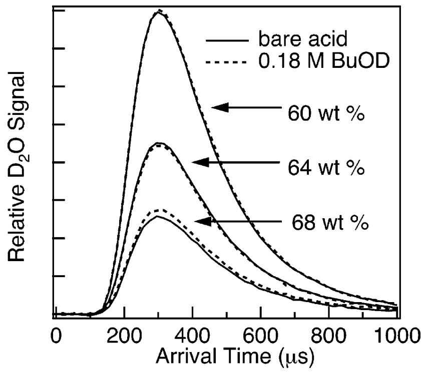

Figure 9. TOF spectra of D_2O evaporation from 60, 64, and 68 wt % D_2SO_4 containing 0 (—) and 0.18 M BuOD (---). The spectra were recorded at $t_{rep} = 0.49$ s, but the spectra appear identical at $t_{rep} = 1.0$ and 0.1 s. These spectra demonstrate that the butyl layer does not impede D_2O evaporation.

replenishes the water that evaporates over the 0.45 s interval, and that no significant cooling occurs over this time. Thus, we believe that the D_2O evaporation flux from the reservoir should be nearly identical to the evaporation flux in an equilibrium environment.

Figure 9 shows our most important result, the comparison of TOF spectra of D_2O evaporating from solutions of 60, 64, and 68 wt % D_2SO_4 containing 0 and 0.18 M BuOD. The evaporation measurements from the bare and butanol-doped acid were recorded 3−5 days apart using replenishment times of 0.10, 0.49, and 1.0 s on each day. In every case, the spectra show that the added butanol has no effect on D_2O evaporation from the acid solutions, at least to within our estimated uncertainty of 5%. Both the intensities and the velocity distributions of the evaporating D_2O remain unaltered. This result is the main topic of the discussion below.

Discussion

Surface Segregation Probed by Hyperthermal Ar Scattering. It is perhaps simplest to explain the unchanged D_2O evaporation from pure and butanol-doped sulfuric acid by postulating that the segregated butyl species lie buried underneath one or a few layers of the acid solution, such that this subsurface layer would not hinder D_2O evaporation from the top solution layers.[35] Surface tension measurements alone do not contradict this picture because a thermodynamic analysis does not determine the atomic-scale location of the surface excess.[56,57]

However, the dramatic differences in hyperthermal argon scattering from pure and butanol-doped acid in Figure 3 argue strongly in favor of an acid surface covered by butyl species (BuOD, $BuOD_2^+$, $BuOSO_3D$, and $BuOSO_3^-$). The changes in Ar scattering are most likely caused by a reduction in the effective surface mass upon covering the SO_4 groups of sulfuric acid with the CH_2 groups of surface butyl species and by increased roughening of the interface by the butyl chains.[25] The lower mass CH_2 groups absorb more of the Ar translational energy per collision than do SO_4 groups, reducing the final energy of the directly scattered Ar atoms and shifting the TOF spectrum to longer times. The incoming Ar atoms also bounce more often along the rougher butyl surface, providing more opportunities for the Ar atoms to dissipate their excess translational energy completely and increasing the fraction of Ar atoms that thermalize and then desorb.[58] This rougher surface may also divert recoiling Ar atoms into a broader angular distribution, thereby lowering the fraction that are measured at the specular angle. We would not expect such dramatic changes in the TOF spectra if the butyl groups were covered by one or more monolayers of D_2O and D_2SO_4. In particular, our previous studies of hyperthermal Ar collisions with a liquid solution of gallium atoms covered by a monolayer of bismuth atoms indicate that the Ar atoms are sensitive only to the outermost bismuth layer.[59] We have also found that hyperthermal Ar collisions with a pure hydrocarbon (squalane) generate TOF spectra similar to those observed in Figure 3 for Ar scattering from the 0.18 M BuOD solutions, suggesting that Ar atoms scatter from surface alkyl chains in a characteristic pattern.[60]

The segregation of butanol to the outermost layer is further supported by interfacial studies of alcohol−water mixtures. Neutron reflectivity measurements indicate that ethanol and butanol in water segregate to the outermost layer,[61] as do molecular dynamics and Monte Carlo simulations.[36,62−64] SFG measurements of alcohol−water mixtures further show that the alkyl groups are oriented outward from the surface, as would be expected in the strongly asymmetric environment of the top surface layer.[49,65−67] On the basis of these studies and the Ar scattering measurements, we conclude that most of the segregated butyl species lie at the surface of the solution, situated with the butyl chains exposed to the vacuum.[68]

Water Evaporation from Bare and Butanol-Doped Sulfuric Acid. Figure 9 demonstrates that butyl species at the surface of 60−68 wt % sulfuric acid do not impede water evaporation. In an attempt to understand why these butyl species remain "invisible", we appeal first to theories describing gas permeation through long-chain surfactants, which typically invoke the notion of free or accessible surface area within the monolayer.[2,69] In these models, gas transport occurs through open areas and fluctuating gaps in the monolayer at the same rate as through the bare liquid, but no evaporation occurs through the intact patches of the film itself, which are assumed to be compact and impermeable. Our surface tension experiments indicate that the butyl film that forms on a 0.2 M butanol solution in 60 wt % D_2SO_4 at 213 K is equivalent to ~80% of the maximum surface coverage (~4×10^{14} cm^{-2}). If this model is applied to films of shorter chain surfactants, then the D_2O evaporation rate should be reduced by roughly a factor of 5 (from α_{bare} to $0.2\alpha_{bare}$), whereas the D_2O evaporation spectra in Figure 9 show that there is no change in evaporation to within our 5% uncertainty (α_{bare} to $0.95\alpha_{bare}$).

To visualize how solute molecules might permeate through butyl films on sulfuric acid, we reproduce in Figure 10 a Monte Carlo simulation of a butanol film on butanol-saturated water computed by Chen, Siepmann, and Klein, also at a surface density of 4×10^{14} cm^{-2}.[62] The side and top views show that the butanol molecules are neither well-ordered nor evenly distributed in the surface film laterally or vertically. The top panel also shows some water penetrating between the butanol chains in the less-dense areas of butanol; the film is quite porous and there are many gaps through which water molecules can pass. Neutron reflectivity measurements yield a width of ~14 Å for this interface, confirming that it is more diffuse than the 7 Å length of an extended butanol molecule.[61]

The porosity inherent in butanol films on water suggests that equivalent density butyl films on sulfuric acid will not achieve the tight packing reached by long-chain surfactants. Within this picture of a porous butyl monolayer, we imagine that D_2O molecules move between the subsurface acid and butyl regions through gaps between the alkyl chains, saturating the film with water. The equality in D_2O evaporation rates of the bare and film-coated acids is then consistent with a picture in which D_2O molecules momentarily residing near the top of the butyl film

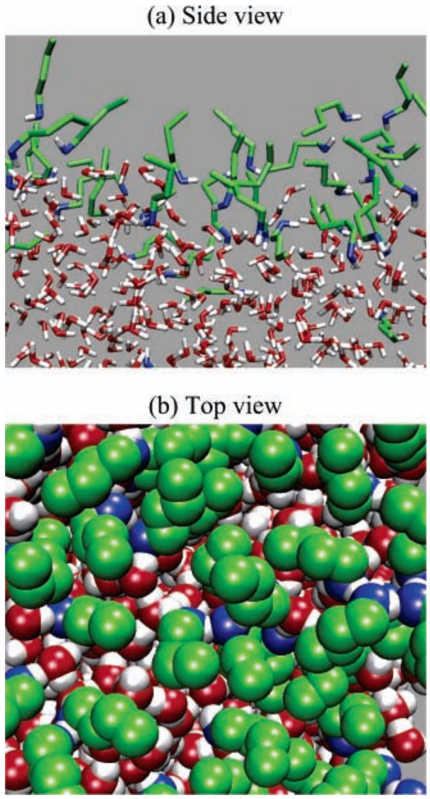

Figure 10. (a) Side and (b) top views of a Monte Carlo simulation of butanol at the surface of water at 298 K. CH_3 groups, CH_2 groups, butanol oxygens, water oxygens, and hydrogens are depicted in green, blue, red, and white, respectively. The united CH_3 and CH_2 groups are 10−20% smaller than actual size. Simulations by B. Chen, J. I. Siepmann, and M. L. Klein based on ref 62.

dissolve back into the acid much more quickly than they desorb into vacuum. In this limit, D_2O becomes fully equilibrated between the acid and film regions and the rate of evaporation is not sensitive to any small barriers for D_2O transport through the butyl film itself. A kinetic scheme for this model is described in ref 70.

We can gain more insight into the equal evaporation rates from the bare and film-coated acids by picturing the reverse D_2O condensation process. An important consequence of the unchanged water evaporation rate is the prediction that the condensation rate into the acid will also be unchanged by the butyl film. At equilibrium, the fluxes of water into and out of the film must be equal, implying that water molecules must enter the bare and butanol-doped acid with the same probability. The entry probability of water into bare 60 wt % D_2SO_4 at 213 K is predicted to be close to 1,[71] further implying that nearly every water molecule in a thermal distribution at 213 K colliding with the butanol-doped acid will become trapped at the surface, permeate fully through the butyl surface layer, and enter the bulk acid.[57] On the basis of Figure 10, we speculate that this complete permeation of D_2O through the butyl film is enforced by its porosity and by attractive forces between D_2O and the alkyl chains and polar headgroups of the butyl species, which at low temperatures should make it difficult for the D_2O to escape back into the vacuum before crossing into the bulk acid. From the perspective of a D_2O molecule colliding with the acid, the butyl film appears porous and sticky, capturing nearly all impinging molecules and transporting them into the acid before they can desorb. Although we have not yet measured the uptake of D_2O into the bare and butanol-doped acids, we show in the following paper that the entry probability of another protic molecule, CF_3CH_2OH, is indeed reduced only slightly by the butyl film.

The equality in D_2O evaporation rates from the bare and film-coated acids must eventually break down as the alkyl chain length increases and cohesive forces make the film more compact and less porous. We find that the addition of 1-hexanol to sulfuric acid indeed creates a hexyl-coated surface that reduces the evaporation of D_2O, indicating that the lengthening of the butyl chain by two CH_2 groups is sufficient to make the segregated film compact and thick enough to impede D_2O transport.[72]

Summary

Butanol is a soluble, short-chain surfactant that segregates to the surface of 60−68 wt % D_2SO_4 supercooled to 213 K, generating films that cover 80% of the surface at bulk concentrations of 0.2 M BuOD. These films have been characterized by hyperthermal argon atom scattering, butanol and water evaporation, and surface tension measurements. The Ar scattering studies show that changes in direct scattering and trapping and desorption track the surface concentration of butyl species extracted from surface tension measurements, allowing the surfactant films to be characterized directly in vacuum. The butanol evaporation measurements further show that a steady evaporation rate is achieved within the 0.5 s replenishment time of the rotating acid-covered wheel, implying that the subsurface and surface regions of the acid closely approach their steady-state butyl compositions.

The most important result of these experiments is the measurement of identical D_2O evaporation rates from the bare and butanol-doped acid at 60, 64, and 68 wt % D_2SO_4 at 213 K. These unchanged rates demonstrate that the butyl films do not impede D_2O transport out of or into the acid, implying that sulfuric acid droplets in the atmosphere coated with short-chain or imperfectly packed surfactants will grow and shrink at their maximum kinetic rates. On the basis of the picture discussed above, we imagine that the butyl species (BuOD, $BuOD_2^+$, $BuOSO_3^-$, and $BuOSO_3D$) form a porous film that allows facile passage of D_2O between the acid and film regions, followed by slow evaporation from the film at a rate that matches D_2O evaporation from the bare acid.[70] In the reverse D_2O absorption pathway, this matching implies that the film is both porous and sticky enough at low temperatures to capture nearly all impinging D_2O molecules and transport them into the acid before they can desorb back into the vacuum.

In the following paper, we show that the unimpeded D_2O evaporation rate is indirectly confirmed by measurements of the nearly unchanged uptake of another protic molecule, CF_3CH_2OH, into bare and butanol-doped sulfuric acid. Furthermore, the entry of HCl and HBr is actually enhanced by the butanol film, in part we speculate because the segregated BuOD molecules provide extra protonation sites at the surface that capture these acidic molecules.

Acknowledgment. We are grateful to the Air Force Office of Scientific Research for supporting this work. We also thank Akihiro Morita and George Zografi for helpful discussions, James Krier for surface tension measurements, and Bin Chen for preparing Figure 10.

Appendix: Diffusion-Limited Replenishment of Butyl Species near the Surface

The replenishment times of the subsurface and surface regions were monitored via BuOD evaporation measurements shown in Figure 6. These times may be estimated from theoretical treatments of diffusion-limited adsorption, which predict that the time required for the concentration $n_{sub}(t)$ just below the surface to asymptotically approach the bulk phase value n_{bulk} is $t \approx (\pi/[4D_{butyl}])(\Gamma/\Delta n_{sub})^2$.[53,73-75] In this equation, Γ is the equilibrium surface excess of butyl species and $\Delta n_{sub} = n_{bulk} - n_{sub}(t)$. The BuOD evaporation flux will reach its final value when $n_{sub}(t) = n_{bulk}$. To estimate when n_{sub} differs from n_{bulk} by the 5% uncertainty of our evaporation measurements, we set Δn_{sub} equal to $0.05n_{bulk}$. The diffusion analysis assumes that the segregated species are confined to a compact outer region, that no barriers exist to the transport of molecules to this region, and that diffusion occurs in the absence of stirring. The diffusion coefficient D_{butyl} is calculated from ref 76 to be 2×10^{-8} cm^2 s^{-1} for 60 wt % D_2SO_4 at 213 K.

The diffusion analysis predicts that, for $n_{bulk} = 1 \times 10^{20}$ cm^{-3} (0.2 M butanol) and $\Gamma = 4 \times 10^{14}$ cm^{-2}, a time of 0.2 s is required to refill the subsurface region to within 5%, whereas the evaporation measurements indicate that replenishment occurs at times shorter than 0.1 s. At the lowest bulk concentration of 0.005 M, we estimate Γ to be $\sim 5 \times 10^{13}$ cm^{-2}.[50] These values yield $t = 4$ s in comparison with an observed time of 1 s. The uncertainties in Δn_{sub}, Γ, and D_{butyl}, however, make us hesitant to conclude that the refilling rate is genuinely faster than predicted. It is possible that an enhanced refilling might arise from mechanical motions of the rotating wheel and scraper, which may mix the acid more efficiently than diffusion in a quiescent solution.

References and Notes

(1) La Mer, V. K.; Healy, T. W.; Aylmore, L. A. G. *J. Colloid Sci.* **1964**, *19*, 673.

(2) Barnes, G. T. *Colloids Surf., A* **1997**, *126*, 149.

(3) Archer, R. J.; La Mer, V. K. *J. Phys. Chem.* **1955**, *59*, 200.

(4) Gaines, G. L. *Insoluble Monolayers at Liquid−Gas Interfaces*; Interscience Publishers: New York, 1966.

(5) Finlayson-Pitts, B. J.; Pitts, J. N. *Chemistry of the Upper and Lower Atmosphere*; Academic Press: New York, 2000.

(6) Carslaw, K. S.; Clegg, S. L.; Brimblecombe, P. *J. Phys. Chem.* **1995**, *99*, 11557. Massucci, M.; Clegg, S. L.; Brimblecombe, P. *J. Phys. Chem. A* **1999**, *103*, 4209. Carslaw, K. S.; Peter, T.; Clegg, S. L. *Rev. Geophys.* **1997**, *35*, 125. Calculations from the aerosol inorganics model at http://mae.ucdavis.edu/wexler/aim.htm.

(7) Jacob, D. *Atmos. Environ.* **2000**, *34*, 2131.

(8) Murphy, D. M.; Thomson, D. S.; Mahoney, T. M. J. *Science* **1998**, *282*, 1664.

(9) Sheridan, P. J.; Brock, C. A.; Wilson, J. C. *Geophys. Res. Lett.* **1994**, *21*, 2587.

(10) Novakov, T.; Hegg, D. A.; Hobbs, P. V. *J. Geophys. Res. Atmos.* **1997**, *102*, 21307.

(11) Middlebrook, A. M.; Murphy, D. M.; Thomson, D. S. *J. Geophys. Res. Atmos.* **1998**, *103*, 16475.

(12) Gill, P. S.; Graedel, T. E.; Weschler, C. J. *Rev. Geophys. Space Phys.* **1983**, *21*, 903.

(13) Toossi, R.; Novakov, T. *Atmos. Environ.* **1985**, *19*, 127.

(14) Seidl, W. *Atmos. Environ.* **2000**, *34*, 4917.

(15) Ellison, G. B.; Tuck, A. F.; Vaida, V. *J. Geophys. Res. Atmos.* **1999**, *104*, 11633.

(16) Mmereki, B. T.; Donaldson, D. J. *J. Phys. Chem. A* **2003**, *107*, 11038.

(17) Rudich, Y. *Chem. Rev.* **2003**, *103*, 5097.

(18) Singh, H.; et al. *J. Geophys. Res. Atmos.* **2000**, *105*, 3795.

(19) Shi, Q.; Davidovits, P.; Jayne, J. T.; Worsnop, D. W.; Kolb, C. E. *J. Phys. Chem. A* **1999**, *103*, 8812.

(20) Hanson, D. R. *J. Phys. Chem. B* **1997**, *101*, 4998.

(21) Barnes, G. T. *Adv. Colloid Interface Sci.* **1986**, *25*, 89.

(22) Langmuir, I.; Schaefer, V. J. *J. Franklin Inst.* **1943**, *235*, 119.

(23) La Mer, V. K. *Retardation of Evaporation by Monolayers: Transport Processes*; Academic Press: New York, 1962.

(24) Morris, J. M.; Behr, P.; Antman, M. D.; Ringeisen, B. R.; Splan, J.; Nathanson, G. M. *J. Phys. Chem. A* **2000**, *104*, 6738.

(25) Nathanson, G. M. *Annu. Rev. Phys. Chem.* **2004**, *55*, 231.

(26) Rubel, G. O. *J. Phys. Chem.* **1987**, *91*, 2103.

(27) Däumer, B.; Niessner, R.; Klockow, D. *J. Aerosol Sci.* **1992**, *23*, 315.

(28) Xiong, J. Q.; Zhong, M. H.; Fang, C. P.; Chen, L. C.; Lippmann, M. *Environ. Sci. Technol.* **1998**, *32*, 3536.

(29) Caskey, J. A.; Barlage, W. B., Jr. *J. Colloid Interface Sci.* **1972**, *41*, 52.

(30) Chang, D. P. Y.; Hill, R. C. *Atmos. Environ.* **1980**, *14*, 803.

(31) Snead, C. C.; Zung, J. T. *J. Colloid Interface Sci.* **1968**, *27*, 25.

(32) For objections to the decanol/water permeation measurements, see: Garrett, W. D. *J. Atmos. Sci.* **1971**, *28*, 816.

(33) Caskey, J. A.; Michelsen, D. L.; To, Y. P. *J. Colloid Interface Sci.* **1973**, *42*, 62.

(34) Schurath, U.; Bongartz, A.; Kames, J.; Wunderlich, C.; Carstens, T. In *Transport and Chemical Transformation of Pollutants in the Troposphere*; Warneck, P., Ed.; Springer: Berlin, 1996; p 182.

(35) Moroi, Y.; Rusdi, M.; Kubo, I. *J. Phys. Chem. B* **2004**, *108*, 6351.

(36) Morita, A. *Chem. Phys. Lett.* **2003**, *375*, 1.

(37) Mmereki, B. T.; Chaudhuri, S. R.; Donaldson, D. J. *J. Phys. Chem. A* **2003**, *107*, 2264.

(38) Williams, L. R.; Long, F. S. *J. Phys. Chem.* **1995**, *99*, 3748.

(39) Klenø, J. G.; Kristiansen, M. W.; Nielsen, C. J.; Pedersen, E. J.; Williams, L. R.; Pedersen, T. *J. Phys. Chem. A* **2001**, *105*, 8440.

(40) Myhre, C. E. L.; Christensen, D. H.; Nicolaisen, F. M.; Nielsen, C. J. *J. Phys. Chem. A* **2003**, *107*, 1979.

(41) Radüge, C.; Pflumio, V.; Shen, Y. R. *Chem. Phys. Lett.* **1997**, *274*, 140.

(42) Baldelli, S.; Schnitzer, C.; Shultz, M. J.; Campbell, D. J. *J. Phys. Chem. B* **1997**, *101*, 10435.

(43) Schnitzer, C.; Baldelli, S.; Shultz, M. J. *Chem. Phys. Lett.* **1999**, *313*, 416.

(44) Fairbrother, D. H.; Johnston, H.; Somorjai, G. *J. Phys. Chem.* **1996**, *100*, 13696.

(45) Lee, D. G.; Demchuk, K. J. *Can. J. Chem.* **1987**, *65*, 1769.

(46) Bonvicini, P.; Levi, A.; Lucchini, V.; Modena, G.; Scorrano, G. *J. Am. Chem. Soc.* **1973**, *95*, 5960.

(47) Deno, N. C.; Newman, M. S. *J. Am. Chem. Soc.* **1950**, *72*, 3852.

(48) Iraci, L. T.; Essin, A. M.; Golden, D. M. *J. Phys. Chem. B* **2002**, *106*, 4054.

(49) See also: Van Loon, L. L.; Allen, H. C. *J. Phys. Chem. B* **2004**, *108*, 17666.

(50) Torn, R. D.; Nathanson, G. M. *J. Phys. Chem. B* **2002**, *106*, 8064.

(51) Jagaber, V. M.; Möhwald, H.; Dutta, P. *Rev. Mod. Phys.* **1999**, *71*, 779.

(52) Lednovich, S. L.; Fenn, J. B. *AIChE J.* **1977**, *23*, 454.

(53) Ward, A. F.; Tordai, L. *J. Chem. Phys.* **1946**, *14*, 453.

(54) The thickness of the depleted region is roughly the depth of solution that must be depleted to repopulate the surface with butyl species, equal to $n_{surf}/n_{bulk} = 400$ Å for a 0.2 M butanol solution and a coverage of $n_{surf} = 4 \times 10^{14}$ cm^{-2}.

(55) The estimate of 10^7 M atm^{-1} is based on solubilities of methanol and ethanol of 2 and 7×10^6 M atm^{-1}, respectively, in 60 wt % H_2SO_4 at 213 K. The methanol value is from ref 48 and the ethanol value is from L. T. Iraci and R. Michelsen, private communication. An evaporation coefficient of 1 was used in estimating the 10 monolayers s^{-1} butanol evaporation rate.

(56) Defay, R.; Prigogine, I. *Surface Tension and Adsorption*; Wiley: New York, 1966; Chapter 2.

(57) The identical velocity distributions of D_2O evaporating from the bare and butyl-coated acid further indicate that the butyl layer does not introduce a change in trapping probability with incident energy over the range of energies in a 213 K thermal distribution. See: Rettner, C. T.; Schweizer, E. K.; Mullins, C. B. *J. Chem. Phys.* **1989**, *90*, 3800.

(58) King, M. E.; Saecker, M. E.; Nathanson, G. M. *J. Chem. Phys.* **1994**, *101*, 2539.

(59) Morgan, J. A.; Nathanson, G. M. *J. Chem. Phys.* **2001**, *114*, 1958.

(60) King, M. E.; Nathanson, G. M.; Hanning-Lee, M. A.; Minton, T. K. *Phys. Rev. Lett.* **1993**, *70*, 1026.

(61) Li, Z. X.; Lu, J. R.; Thomas, R. K.; Rennie, A. R.; Penfold, J. *J. Chem. Soc., Faraday Trans.* **1996**, *92*, 565.

(62) Chen, B.; Siepmann, J. I.; Klein, M. L. *J. Am. Chem. Soc.* **2002**, *124*, 12232.

(63) Daiguji, H. *Microscale Thermophys. Eng.* **2002**, *6*, 223.

(64) Tarek, M.; Tobias, D. J.; Klein, M. L. *J. Chem. Soc., Faraday Trans.* **1996**, *92*, 559.

(65) Ma, G.; Allen, H. C. *J. Phys. Chem. B* **2003**, *107*, 6343.

(66) Ju, S. S.; Tzong-Daw, W.; Yeh, Y.-L.; Wei, T.-H.; Huang, J.-Y.; Lin, S. H. *J. Chin. Chem. Soc.* **2001**, *48*, 625.

(67) Allen, H. C.; Raymond, E. A.; Richmond, G. L. *J. Phys. Chem. A* **2001**, *105*, 1649.

(68) The Ar scattering and BuOD evaporation studies demonstrate that the surface and subsurface butyl concentrations have reached their terminal values, but they do not prove that the packing and conformations of the surface butyl species have relaxed to their equilibrium distributions.

Replenishment times exceeding the longest 1.0 s time used here may lead to more equilibrated films, but in this case we ask why even a partially relaxed film does not impede gas transport. Dynamic surface tension measurements may be helpful in characterizing the longest relaxation time. See: Zhmud, B. V.; Tiberg, F.; Kizling, J. *Langmuir* **2000**, *16*, 7685.

(69) Blank, M. *J. Phys. Chem. A* **1964**, *68*, 2793.

(70) We analyze the kinetic schemes $D_2O_{acid} \underset{k_{-1}}{\overset{k_1}{\rightleftarrows}} D_2O_{film} \xrightarrow{k_2} D_2O_{gas}$ for the film-coated acid and $D_2O_{acid} \xrightarrow{k_0} D_2O_{gas}$ for the bare acid. The rate constants k_1 and k_{-1} refer to transport of D_2O between the subsurface acid and the top of the butyl film, and k_2 and k_0 refer to D_2O desorption from the top of the film into vacuum and the surface of the bare acid into vacuum, respectively. When the barriers to D_2O transport through the film are small, k_{-1} should be much greater than k_2, and D_2O will establish equilibrium between the acid and film regions. The rate of water evaporation then equals $k_2K_{eq}[D_2O]_{acid}$, where $K_{eq} = \exp(-\Delta G^\circ_{acid\leftrightarrow film}/RT)$. We also assume that there are no barriers to desorption of D_2O from the top of the butyl film beyond the free energy difference between the top of the film and the gas phase, $\Delta G^\circ_{film\leftrightarrow gas}$, or from the surface of the bare acid beyond the free energy difference $\Delta G^\circ_{acid\leftrightarrow gas}$. In these cases, the ratio of desorption rates from the film-coated and bare acids is $(k_2/k_0)K_{eq} = \exp(-[\Delta G^\circ_{film\leftrightarrow gas} - \Delta G^\circ_{acid\leftrightarrow gas}]/RT)K_{eq}$, which equals 1 upon substitution for K_{eq}. This equality occurs because the barriers to D_2O transport through the film are small enough that $k_2 \ll k_{-1}$; the film is porous yet sticky enough to make the rate of transport of D_2O from the film into the acid much faster than the rate of evaporation into the vacuum.

(71) Gershenzon, M.; Davidovits, P.; Williams, L. R.; Shi, Q. A.; Jayne, J. T.; Kolb, C. E.; Worsnop, D. R. *J. Phys. Chem. A* **2004**, *108*, 1567. The uptake of H_2O into 62 wt % H_2SO_4 at 213 K is estimated to be greater than 0.85.

(72) Glass, S. V.; Park, S. C.; Nathanson, G. M. To be submitted for publication.

(73) Mysels, K. *J. Phys. Chem.* **1982**, *86*, 8648.

(74) Hansen, R. S. *J. Phys. Chem.* **1960**, *64*, 637.

(75) Fainerman, V. B.; Makievski, A. V.; Miller, R. *Colloids Surf.* **1994**, *87*, 61.

(76) Klassen, J. K.; Hu, Z. J.; Williams, L. R. *J. Geophys. Res. Atmos.* **1998**, *103*, 16197.